Plane Slider Bearing Load Due to Fluid Inertia—Experiment and Theory

J. A. Tichy

S.-H. Chen

Department of Mechanical Engineering, Aeronautical Engineering & Mechanics, Rensselaer Polytecnhic Institute, Troy, N.Y. 12181

Experimental measurements of load in a simulated plane slider bearing have been performed. The flow is laminar but modified Reynolds numbers up to 30 are obtained. In comparison with actual bearings, large film thickness and slow velocity are used to avoid experimental difficulties and isolate the inertia effect. The load is found to have increased by 100 percent relative to lubrication theory at modified Reynolds number about ten. Most existing inertia theories predict only a small effect at this Reynolds number. A simple theory is proposed to account for this discrepancy, combining existing models which have considered an inlet pressure jump and small Reynolds number perturbation analysis.

Introduction

The effect of fluid inertia in hydrodynamic lubrication has been the subject of speculation and analysis for many years, both the laminar and turbulent flow cases. A rather large body of experimental literature also exists but is outnumbered by analytical papers in a ratio of at least four to one. The present paper presents global experimental measurements of normal loading force in a plane slider bearing operating in the laminar regime, but at modified Reynolds numbers of order one and greater, where fluid inertia forces may be significant. We are not aware of any other such data in the literature. A simple theory is also presented in support of the experimental results.

Lubrication theory is strictly applicable when the inertia terms of the Navier-Stokes equations are negligibly small. There are three conditions which may arise when inertia terms are significant: (1) centrifugal instabilities (Taylor vortices), (2) parallel flow instabilities resulting in so-called Tollmien-Schlichting waves and eventually turbulence, and (3) a stable laminar flow state which differs from lubrication flow. Each is characterized by a different Reynolds number. The former two produce no measurable macroscopic effect in fully developed flow until the sudden onset of the instability, while the third produces a continuous change in the force as Reynolds number increases.

The review article of Saibel and Macken [1] lists pertinent experimental literature to 1974. Most of these articles are concerned with Taylor vortex flows in classical fluid mechanics, rather than bearing studies. The first studies of bearings are due to Wilcock in 1950 [2], and Smith and Fuller in 1956 [3]. Both articles are concerned with turbulence in journal bearings. (If the film curvature is low, i.e., if journal bearing films are thin; turbulence is a more likely outcome of high journal bearing speed than centrifugal instabilities.) Abramovitz [4] first studied turbulence in tilting pad thrust bearings in 1956. In a series of articles by Orcutt et al. [5, 6, 7] experimental results were published for partial pad arc bearings, full journal bearings and tilting pad journal bearings in laminar and turbulent flow and under steady and dynamic conditions. An entire issue of the *Journal of Lubrication Technology*, January 1974, was concerned with bearing turbulence. A number of articles in this issue reported on experimental measurements: Smalley et al. [8] (step journal); Galetuse [9] (a flow between a plane and a circular surface); Burton, Carper and Hsu [10] (tilted pad bearing); and Gregory [11] (tilted pad bearing). In all cases the emphasis is on turbulent flow.

Transition to turbulence begins when the Couette Reynolds number defined as

$$\mathrm{Re} = \frac{Uh_0}{\nu}$$

reaches a critical value Re_{cr} = 1000–2000, where U is a reference longitudinal (sliding) speed, h_0 is a reference film thickness and ν is the lubricant kinematic viscosity. The fluid inertia effect is governed by the reduced Reynolds number:

$$\mathrm{Re}^* = \mathrm{Re}\frac{h_0}{B},$$

where B is a bearing reference breadth (in the direction of flow). For lubrication theory $\mathrm{Re} < Re_{cr}$ (but probably $\mathrm{Re} \gg 1$) and $\mathrm{Re}^* \ll 1$. If $\mathrm{Re} > \mathrm{Re}_{cr}$, turbulence will result, regardless of the value of Re^*. This is the case in all of the above studies. However, if $\mathrm{Re} < \mathrm{Re}_{cr}$ but Re^* is *not* much less than one, the fluid inertia effect may be significant. To our knowledge, this condition has not been studied experimentally.

Applications in which such conditions may arise are very high speed bearings with low viscosity conventional lubricants, or specialized applications where a low viscosity working fluid must also serve as a lubricant. Examples of the latter are cryogenics (liquified gases), liquid metals, or water. In a very high speed pad bearing consider conditions where B = 6 cm, h_0 = 0.02 cm, U = 4000 cm/s, ν = 01 cm^2/s, which

Contributed by the Tribology Division of The American Society of Mechanical Engineers and presented at the ASME/ASLE Joint Lubrication Conference, San Diego, Calif., October 22–24, 1984. Manuscript received by the Tribology Division, November 23, 1983. Paper No. 84-Trib-9.

gives Re = 800, Re* = 2.7. The above parameters might be in force for a lightly loaded six pad thrust bearing, 16 cm shaft diameter, with a light turbine oil at 70°C.

Let us skip briefly to the final conclusion of this study: fluid inertia forces may contribute significantly to load capacity, due to inlet pressure conditions, in the range of modified Reynolds number where previously the effect was thought to be small. Inlet pressure conditions have been considered by Pan [12], Constantinescu et al. [13] and Tipei [14]. Experimental pressures for turbulent flow have been reported by Burton and Carper [15]. References [12–14] contain detailed analyses of the zone outside the bearing, making certain assumptions regarding flow profiles and free surface geometry. The theoretical studies emphasize the immediate inlet zone of the bearing rather than the full pressure profiles. These articles report a pressure head at the inlet, referred to a Bernoulli pressure $\rho U^2/2$ (where ρ is the fluid density). In the present article we simply summarize the inlet pressure condition with a loss coefficient k, rather than perform such detailed calculations at the inlet.

Launder and Leschziner [16] and Elrod [17] performed numerical analyses of the effect of fluid inertia in finite plane slider bearings. In both cases the momentum is averaged across the film. Elrod endorsed the proposed concept of an inlet pressure jump but results are presented only for the case of a fixed ambient inlet pressure.

Analysis

Consider the steady sliding two-dimensional laminar flow of a lubricating film (see Fig. 1). After applying order-of-magnitude estimates and omitting body forces, the governing continuity and momentum equations for the incompressible flow of a Newtonian fluid are

$$\frac{\partial u}{\partial x} + \frac{\partial v}{\partial y} = 0, \tag{1a}$$

$$\rho\left(u\frac{\partial u}{\partial x} + v\frac{\partial u}{\partial y}\right) = -\frac{\partial p}{\partial x} + \mu\frac{\partial^2 u}{\partial y^2}, \tag{1b}$$

$$0 = \frac{\partial p}{\partial y}, \tag{1c}$$

with boundary conditions,

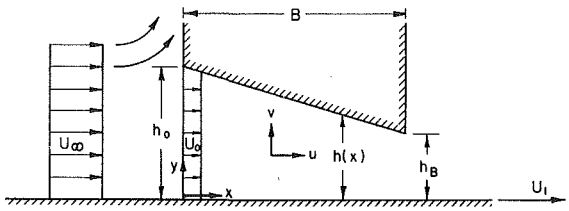

Fig. 1 Plane slider bearing geometry

$$u = U \quad \text{at} \quad y = 0 \tag{2a}$$

$$u = 0 \quad \text{at} \quad y = h(x) \tag{2b}$$

$$p = p_a \quad \text{at} \quad x = B \tag{2c}$$

$$p = p_0 \quad \text{at} \quad x = 0. \tag{2d}$$

We include the effect of fluid inertia but invoke the thin film assumptions to obtain equation (1). Various symbols used are described in the Nomenclature.

Here p_0 is a pressure jump at the entrance region due to the Bernoulli effect. Assuming uniform upstream conditions and a uniform velocity profile at the entrance region, the Bernoulli equation including a loss coefficient k is used here to account for the inlet pressure jump:

$$p_a + \frac{1}{2}\rho U_\infty^2(1-k) = p_0 + \frac{1}{2}\rho U_0^2 \tag{3}$$

where U_0 is the uniform velocity at the inlet, and U_∞ is the velocity far upstream of the bearing. In this analysis, the far upstream variables p_a and U_∞ are considered to be known beforehand, but the inlet pressure p_0, see equation (2*d*), is found by coupling the global flow rate,

$$\int_0^h u\, dy = \text{const} = U_0 \tag{4}$$

with equation (3). Equation (4) is obtained readily by integrating equation (1*a*) across the film, and integrating the resulting equation with respect to x.

Defining dimensionless quantities:

Nomenclature

B = bearing breadth (in x-direction), see Fig. 1
h = film thickness, Fig. 1
h_0 = inlet film thickness, Fig. 1
h_B = exit film thickness, Fig. 1
k = loss coefficient
L = bearing length (normal to paper)
m = slope variable $= -(h_0 - h_B)/h_0$
p = pressure
p^* = dimensionless pressure $= (p - p_a)h_0^2/\mu B U_1$
p_a = ambient fluid pressure
p_0 = inlet pressure
p_0^* = dimensionless inlet pressure $= (p_0 - p_a)h_0^2/\mu B U_1$
Re = Couette Reynolds number $= \rho U_1 h_0/\mu$
Re* = modified Reynolds number $= \text{Re}^* h_0/B$
u = fluid velocity in the x-direction
u^* = dimensionless fluid velocity in the x-direction $= u/U_1$
U_1 = bearing slider velocity, Fig. 1
U_∞ = reference upstream fluid velocity, Fig. 1
U_0 = fluid velocity at inlet, Fig. 1
U_∞^* = dimensionless upstream fluid velocity $= U_\infty/U_1$
U_0^* = dimensionless inlet fluid velocity $= U_0/U_1$
v = fluid velocity in the y-direction
v^* = dimensionless fluid velocity in the y-direction
x = coordinate axis along film, Fig. 1
x^* = dimensionless coordinate axis $= x/B$
y = coordinate axis across film, Fig. 2
y^* = dimensionless coordinate axis $= y/h_0$
W = load $= L\int_0^B P\, dx = (\mu U_1 B^2 L/h_0^2)W^*$
W^* = dimensionless load $= \int_0^1 P^* dx^*$
ρ = fluid density
μ = fluid viscosity

Subscripts

0 = inlet region
l = lubrication theory (zero order) solution
R = Reynolds number (first order) perturbation
* = dimensionless variable

$$u^* = \frac{u}{U_1}, \; v^* = \frac{vB}{U_1 h_0}, \; x^* = \frac{x}{B}, \; y^* = \frac{y}{h_0},$$

$$p^* = \frac{(p - p_a) h_0^2}{\mu B U_1}, \tag{5}$$

the following governing dimensionless equations are obtained by substituting equations (5) into equation (1):

$$\frac{\partial u^*}{\partial x^*} + \frac{\partial v^*}{\partial y^*} = 0$$

$$\mathrm{Re}^* \left(u^* \frac{\partial u^*}{\partial x^*} + v^* \frac{\partial u^*}{\partial y^*} \right) = - \frac{\partial p^*}{\partial x^*} + \frac{\partial^2 u^*}{\partial y^{*2}}$$

$$0 = \frac{\partial p^*}{\partial y^*}. \tag{6}$$

The modified or reduced Reynolds number $\mathrm{Re}^* = \rho U_1 h_0^2 / \mu B$, occasionally referred to only as Reynolds number, arises naturally from the scaling of equation (5). Also, substituting successively equations (3) and (5) into equation (2) yields the corresponding boundary conditions:

$$\begin{aligned} u^* &= 1 \quad \text{at} \quad y^* = 0 \\ u^* &= 0 \quad \text{at} \quad y^* = 1 + mx^* \\ u^* &= 0 \quad \text{at} \quad x^* = 1 \\ p_0^* &= \frac{1}{2} \mathrm{Re}^* [U_\infty^{*2} (1 - k) - U_0^{*2}] \quad \text{at} \quad x^* = 0 \end{aligned} \tag{7}$$

where $m = -[h_0 - h_B]/h_0$ is a slope variable in dimensionless representation. We now are considering only the plane slider bearing which corresponds to the experimental apparatus, however, the method presented is quite general for any $h(x)$.

A first-order Reynolds number regular perturbation analysis following that described by Pinkus and Sternlicht [18] is used here to linearize the inertial terms in the longitudinal momentum equation. We set

$$\begin{aligned} u^* &= u_l^* + \mathrm{Re}^* u_R^* + 0(\mathrm{Re}^{*2}) \\ v^* &= v_l^* + \mathrm{Re}^* u_R^* + 0(\mathrm{Re}^{*2}) \\ p^* &= p_l^* + \mathrm{Re}^* p_R^* + 0(\mathrm{Re}^{*2}) \end{aligned} \tag{8}$$

where the l subscript denotes the lubrication theory case (zero-order perturbation) and R the improvement due to inertia (first-order perturbation). Although the above process is strictly true for $\mathrm{Re}^* \ll 1$, it is well known to be suitable for $\mathrm{Re}^* \sim 0(1)$ due to fortunate rapid convergence of the higher order terms.

The zero-order and first-order differential equations and velocity boundary conditions follow exactly as reported in Pinkus and Sternlicht. The pressure boundary conditions are somewhat different:

$$\begin{aligned} \mathrm{Re}^{*0}: \quad & p_l^* = 0 \quad \text{at} \quad x^* = 1 \\ & p_l^* = 0 \quad \text{at} \quad x^* = 0 \\ \mathrm{Re}^{*1}: \quad & p_R^* = 0 \quad \text{at} \quad x^* = 1 \\ & p_{R0}^* = \frac{1}{2} [U_\infty^{*2} (1 - k) - U_{0l}^{*2}]. \end{aligned} \tag{9}$$

Note that the lubrication flow rate U_{0l}^* determines the inertia inlet pressure jump p_{R0}.

The pressure field can be obtained after considerable manipulation:

$$p_l^*(x^*) = \frac{6(m+1)}{m(m+2)} \frac{1}{(1+mx^*)^2} - \frac{6}{m} \frac{1}{(1+mx^*)} + \frac{6}{m(m+2)}$$

$$p_R^*(x^*) = F_1(m,k) \frac{1}{(1+mx^*)^2} + F_2(m,k) \frac{1}{(1+mx^*)} + F_3(m,k) \ln(1+mx^*) + F_4(m,k)$$

$$F_1(m,k) = \frac{(m+1)^2}{m(m+2)} \left\{ - \frac{3}{35} \frac{m}{m+2} - \frac{1}{7} \ln(1-m) - \frac{1}{2} \frac{(m+1)^2}{(m+2)^2} + \frac{1}{2} (1-k) \right\}$$

$$F_2(m,k) = \frac{3}{35} \left(\frac{m+1}{m+2} \right); \quad F_3(m,k) = - \frac{1}{7}$$

$$F_4(m,k) = -F_1(m,k) - \frac{3}{35} \left(\frac{m+1}{m+2} \right) - \frac{1}{2} \left(\frac{m+1}{m+2} \right)^2 + \frac{1}{2} (1-k). \tag{10}$$

By integrating equation (10) the dimensionless load capacity is obtained:

$$W_l^* = \int_0^1 p_l^*(x^*) dx^* = \frac{6}{m^2} \left[\frac{2m}{m+2} - \ln(1+m) \right]$$

$$W_R^* = \int_0^1 p_R^*(x^*) dx^* = \frac{1}{(1+m)} F_1(m,k) + \frac{1}{m} \ln(1+m) F_2(m,k) + \frac{1}{m} [(1+m)\ln(1+m) - m] F_3(m,k) + F_4(m,k). \tag{11}$$

The total load capacity in dimensional form is

$$W = \frac{\mu U_1 B^2 L}{h_0^2} (W_l^* + \mathrm{Re}^* W_R^* + \ldots). \tag{12}$$

Some typical values obtained from equations (10)–(12) are listed in Table 1. The far upstream velocity U_∞ has been set equal to U_1, the sliding velocity. This would seem to best simulate the simple thrust pad bearing condition where lubricant is carried along the runner (the rotating shaft end), until it encounters the pad. At that location some fluid enters the bearing wedge and some is deflected away, as described in references [12–14].

From equation (7) it is clear that the result obtained by Pinkus and Sternlicht is a special case of the authors' solution with k equal to $1 - U_0^2/U_\infty^2$, i.e., $p_0 = 0$. There does not seem to be a compelling reason to support this assumption. For entry flow in a pipe or channel, there is a well-known entrance pressure loss due to convective acceleration of fluid into the passage. The effect described here is physically similar, but there may be an entrance loss or gain depending on whether fluid is accelerated or decelerated into the bearing gap.

The slope variable m is defined such that for $m = -0.5$, the bearing exit gap is one-half the entrance. As the absolute value of the slope decreases, the inertia load becomes greater relative to the viscous lubrication load. As the loss coefficient

Table 1 Dimensionless load for various inlet loss coefficients

Slope m	Lub. Load W_l	Inertia load W_R^* ref. [16]	Inertia load W_R^* $k=0.3$	Inertia load W_R^* $k=0.5$	Inertia load W_R^* $k=0.8$
−0.833	3.1379	0.0588	0.3517	0.2660	0.1374
−0.667	1.3312	0.0283	0.2674	0.1924	0.0799
−0.500	0.6355	0.0123	0.2086	0.1420	0.0420
−0.333	0.2951	0.0044	0.1664	0.1064	0.0164

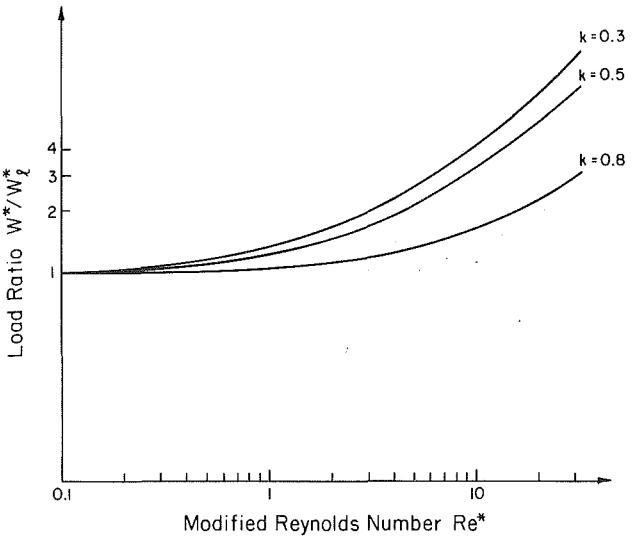

Fig. 2 Theoretical variation of load with Reynolds number and loss coefficient

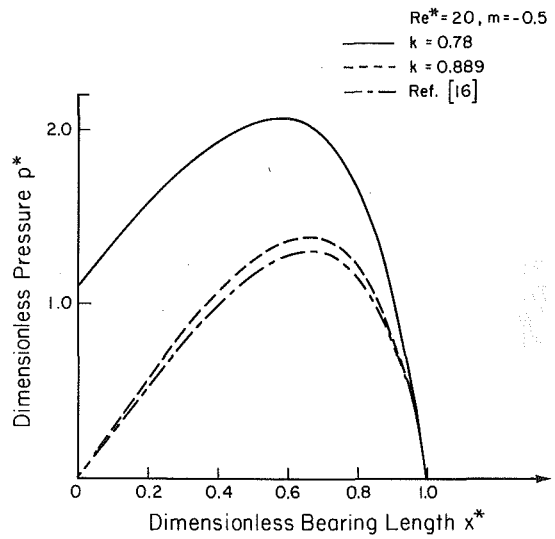

Fig. 4 Comparison of the present results with Launder and Leschziner [16]

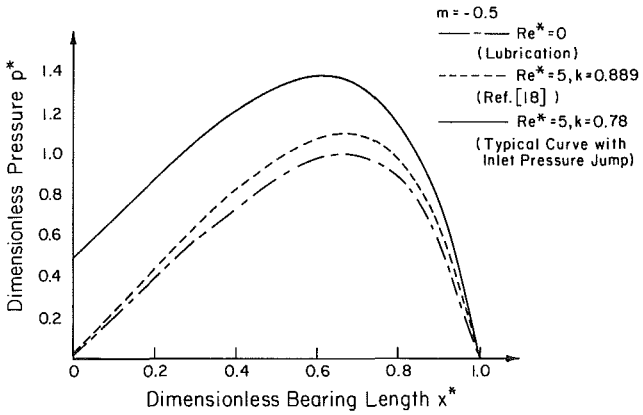

Fig. 3 Theoretical pressure profiles; Re* = 0., 5.; k = 0.78, 0.89

increases, the inertia load W_R decreases. For the inlet pressure jump to be zero, the loss coefficient becomes

$$k = 1 - \frac{U_0^2}{U_\infty^2} = 1 - \left(\frac{1+m}{2+m}\right)^2. \tag{13}$$

Hence for $m = -0.5$, the loss coefficient is very large, k = 0.889, meaning that almost all the incoming dynamic head has been dissipated. From the calculations of inlet pressure jumps in references [12–13] an equivalent loss coefficient can be easily determined. It turns out in both cases that k is approximately 0.3.

Figure 2 shows the variation of the ratio of the nondimensional load capacity W/W_l ratio versus Reynolds number Re* for different values of the loss coefficient k. Over a wide range of k there is a significant increase of load capacity for modified Reynolds number of order one. The occurrence of this phenomenon is due to the entrance pressure jump, which may dominate the entire pressure field, see Fig. 3. The curve shown for k = 0.78, computed from equation (10), turns out to be the best fit value for the experimental data presented below.

The present results are compared with those obtained by Launder and Leschziner [16] for a very long finite bearing in Fig. 4. Appropriate changes have been made for different definitions of modified Reynolds number and dimensionless pressure. Three cases are shown: (1) results from reference [16]; (2) results from the pressure analysis, forcing the inlet pressure to ambient with a loss coefficient k = 0.889; and (3) results from the present analysis using the "best fit" value k = 0.78. The agreement between cases (2) and (3) is excellent.

Apparatus and Procedure

The objective of the experiment is to measure the relation between modified Reynolds number Re* and dimensionless total load W^*, i.e., the effect of fluid inertia on bearing load capacity. In comparison with real bearing cases, large film thickness and slow velocity are used here to avoid experimental difficulties. However, dynamic similitude between the model (the experiment rig) and the prototype (the real-world bearing) is maintained.

We seek here to isolate the inertia effect rather than reconstruct the more complex "real world." Establishing a clear relationship between Reynolds number and fluid film forces would be an extremely difficult task in an actual bearing. Any number of intervening variables separately or in combination could obscure the results. Such possible variations are machining and alignment inaccuracies, frictional heating, elastic distortion of surfaces and three-dimensional effects. In addition, the equipment necessary to produce the speeds and forces required are not suitable for a laboratory bench type experiment.

A photograph and schematic drawing of the entire experimental apparatus are shown in Figs. 5 and 6. Figure 7 depicts the mechanical assembly used to simulate the flow in an infinite plane slider bearing and measure the fluid film force. Some parameters of the apparatus are listed in Table 2.

The bearing gap to width ratio is 0.1 at the inlet, 0.05 at the exit. These are maximum conditions for the experiments conducted. It appears that the thin film assumption $h \ll B$ can be applied (but just barely). Hays [19] has pointed out that for $L/B > 3$, the flow in a plane slider bearing is nearly two-dimensional, and the reduction in load capacity per unit length is less than 20 percent relative to the infinite bearing case. Hence it would also seem satisfactory to apply the two-dimensional flow assumption here. Once these conditions (assumptions) have been invoked, the only dimensionless parameters of the problem are the modified Reynolds number and the slope parameter m, cf. equations (6) and (7). Therefore, to maintain dynamic similitude, equality of these two parameters must be maintained between "model" and

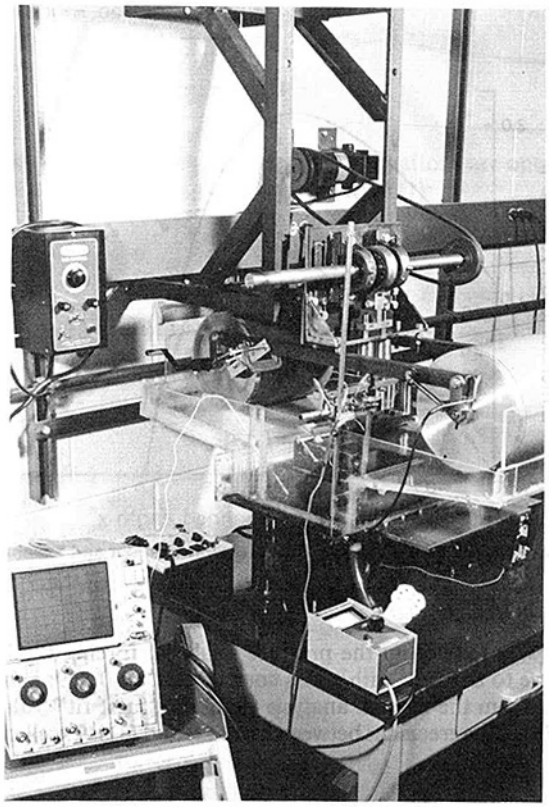

Fig. 5 Photograph of apparatus

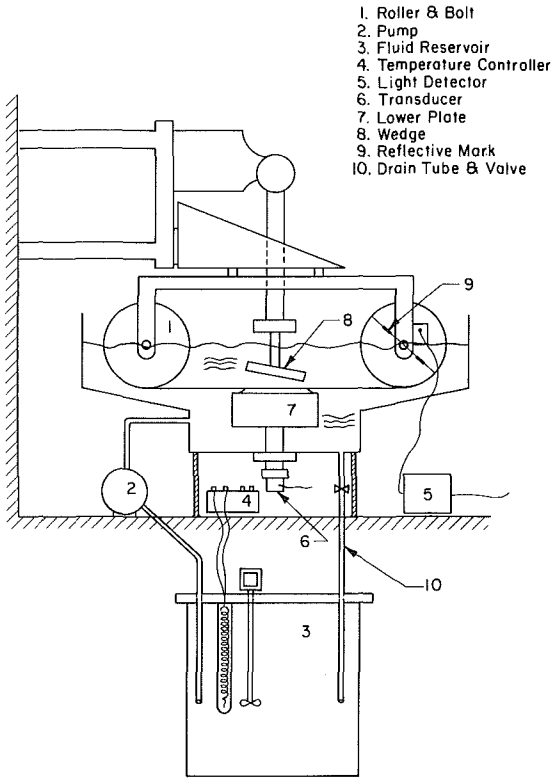

Fig. 6 Schematic drawing of experimental apparatus

"prototype." In actual bearings $m = -0.5$ is a typical value, and is used in the present experiment. The modified Reynolds number is less than one in most applications, but may attain values of 10–20 in specialized applications with low viscosity lubricants or at very high speeds.

Table 2 Kinematic parameters of the bearing rig

Width of plate B	5.08 cm
Length of plate L	17.4 cm
Diameter of roller d	20.32 cm
Inlet gap opening h_0	0.508 cm (maximum)
Exit gap opening h_B	0.254 cm (maximum)
Maximum sliding velocity U_1	100 cm/s

Table 3 Properties of test fluids at experiment temperatures

Fluid	Density ρ (gr/cm^3)	Kinematic viscosity ν (cm^2/s)	Temperature
50 W	0.9	5.00	(25.6°C)
20 W	0.88	1.55	(24.4°C)
		0.93	(33.6°C)
No. 10	0.85	0.48	(21.1°C)
No. 6	0.833	0.18	(22.2°C)

The bearing runner is simulated by a thin (0.03 cm) continuous fabric belt. The belt is driven by a pair of large hand-cranked rollers. The belt is about 10 m in length, and as the crank is turned the belt winds from one roller to the other. Hence the length of a test is about 10 s, then the belt must be rewound. A good deal of effort was spent trying to develop a belt loop driven by a motor. The bearing fluid film forces developed are very small and the extraneous vibration and noise introduced by the motor and drive system could not be reduced to acceptable levels. The present rotating drums and belt are supported completely independently of the bearing wedge and lower plate. Hence the mechanical noise due to hand turning the crank has very little effect on the measured signal.

The rollers are adjusted until when the belt is pulled tight without any creases, the lower plane of the belt just touches the lower bearing plate. When pressure is developed within the gap, the belt presses against the lower plate and this force is sensed by the transducer. The shaft which connects the lower plate to the force transducer is supported on axial roller bearings. These bearings take up moments on the lower bearing plate, but do not exert any force in the direction normal to the plate. Therefore the transducer senses only the bearing normal force due to the fluid pressure.

Two small pieces of reflective paper attached to the roller and a light detector linked to the oscilloscope are used to provide the belt revolution time. Since the roller diameter is known, the belt surfce velocity can be calculated.

A strain gage force transducer is used to measure the load generated within the fluid film. The transducer is a Sundstrand model 923F Load Cell connected to a Sundstrand Model 503D charge amplifier. The maximum sensitivity is 0.073 V/N. The bearing forces are extremely small, between 0.1 and 1.0 N, therefore a high resolution signal is required. The transducer is mounted to the lower bearing pad and its signal sent to the oscilloscope, so that the total load W can be measured.

A temperature control system is used to maintain the fluid temperature at a desired value for viscosity variation. A tank which is an integral part of the bearing mechanical assembly contains fluid which serves both as the test sample itself and a constant temperature bath. The system also includes a set of heating elements submerged in an external fluid reservoir, plus an adjustable pump and a drain tube which permit fluid flow into and out of the bearing assembly tank. The temperature control takes place in the external reservoir, but the temperature in the tank is carefully measured at several locations. As a rule the reservoir and bearing assembly tank

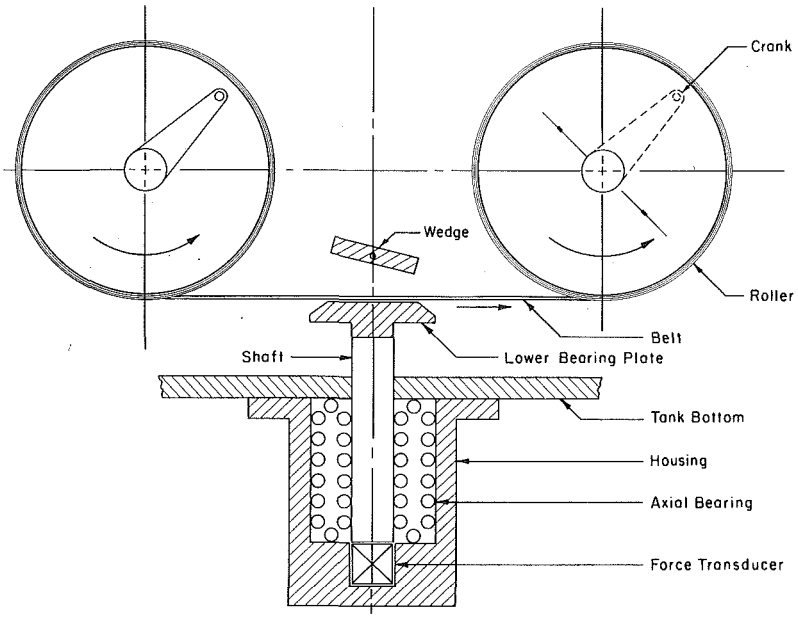

Fig. 7 Schematic drawing of bearing rig mechanical components

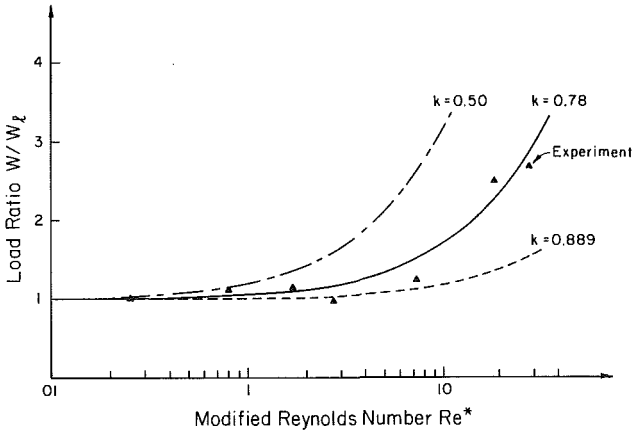

Fig. 8 Variation of load with Reynolds number, experiment and theory

temperatures are slightly different at steady state. The flow rate is contolled by the pump and a valve connected to the drain tube. Before proceeding with the test, the temperature control system is put into operation until the fluid reaches a thermodynamic steady temperature, and then conditions are maintained in this state throughout a series of tests. Rotation of the drums provide vigorous mixing of the fluid sample.

Four different oils were used as test fluids in the series of experiments. Two are straight grade commercial automotive engine oils (20 W and 50 W). The two others are low viscosity commercial spindle oils (No. 6 and No. 10). The density and viscosity at certain temperatures of these fluids are listed in Table 3. Viscosities at the test temperatures were measured in a capillary viscometer by standard techniques.

Results

The maximum Couette Reynolds number Re is 600. so the flow is always laminar. Eight values of Re* were chosen between 0.2 and 30. For each point a suitable fluid, temperature and belt sliding velocity were selected. In the vicinity of each point, the test was repeated 20 times, attempting to duplicate conditions as nearly as possible. The reason for this procedure is that the bearing forces were generally very small. The mechanical noise and drift of the electrical signal were often significant. The mechanical noise came from small extraneous forces of the belt against the plate, sloshing of fluid in the tank, etc. The drift was due to the high amplification gain on the transducer signal.

By using statistical methods, the value of dimensionless load W at each Re was found. To better account for the noise, the procedure was also repeated at the same conditions with the upper pad taken away. The difference between these two values can be treated as the force generated within the fluid film.

Figure 7 shows the final result of the experiments. When the loss coefficient is taken as 0.78, there is a good agreement between the theory and the measured values. Each experimental point shown in the mean of twenty tests. In the worst case, the standard deviation in load ratio is 13 percent for the twenty tests.

Discussion and Conclusions

An approximate solution of Navier-Stokes equation has been presented for determining the pressure field and load capacity in an infinite slider bearing including the fluid inertia effect. The analysis is based on linearizing the inertia terms by using a low Reynolds number perturbation method proposed by Pinkus and Sternlicht. Instead of using ambient pressure at the entrance as a boundary condition, the present authors propose that a pressure jump exists at the inlet, caused by the Bernoulli effect.

To better generalize the problem, the Bernoulli equation including a loss coefficient is used to account for the pressure jump. It turns out that the jump is of the order Re* relative to the viscous pressure generated in the bearing. Unless the loss coefficient is very near to $1 - U_0^2 \approx 8/9$, the effect of the pressure jump may dominate the entire pressure field. Consequently a large correction to the lubrication theory is found at fairly moderate modified Reynolds number.

Experimental evidence is given to support the theoretical results. Data collected from experimental apparatus show that the theory predicts the correct trend and correctly predicts a significant increase in load capacity.

Perhaps a better persepective from which to consider these results is that the experiments clearly show a significant effect

of fluid inertia (100 percent increase in load) at conditions where previously the inertia effect was thought to be small (modified Reynolds number of ten). A theory is proposed which suggests that this result is attributable to an inlet pressure jump, caused by the Bernoulli effect as fluid (moving at the speed of the runner) is decelerated into the bearing. Although the present apparatus differs greatly from a real bearing situation, it seems reasonable that such inlet phenomena may be important there also.

Acknowledgment

The research described herein was funded by the United States National Science Foundation, Grant No. MEA 80-18028, Dr. Elbert Marsh, Program Manager. This support is gratefully acknowledged.

References

1 Saibel, E. A., and Macken, N. A., "Nonlaminar Behavior in Bearing: A Critical Review of the Literature," ASME JOURNAL OF LUBRICATION TECHNOLOGY, Vol. 96, No. 1, 1974, pp. 174–181.

2 Wilcock, D. F., "Turbulence in High Speed Journal Bearings," *Trans. ASME*, Vol. 72, 1950, pp. 825–833.

3 Smith, M. I., and Fuller, D. D., "Journal Bearing Operation at Superlaminar Speeds," *Trans. ASME*, Vol. 78, 1956, pp. 469–474.

4 Abramovitz, S., "Turbulence in a Tilting Pad Thrust Bearing," *Trans. ASME*, Vol. 78, 1956, pp. 7–11.

5 Orcutt, F. K., "Investigation of a Partial Arc Pad Bearing in the Superlaminar Flow Regime," ASME *Journal of Basic Engineering*, Vol. 87, No. 2, 1965, pp. 145–152.

6 Orcutt, F. K., and Arwas, E. B., "The Steady-State and Dynamic Characteristics of a Full Circular Bearing and a Partial Arc Bearing in the Laminar and Turbulent Flow Regimes," ASME JOURNAL OF LUBRICATION TECHNOLOGY, *Trans. ASME*, Vol. 89, No. 3, 1967, p. 392.

7 Orcutt, F. K., and Ng, C. W., "Steady-State and Dynamic Properties of the Floating-Ring Journal Bearing," ASME JOURNAL OF LUBRICATION TECHNOLOGY, Vol. 90, No. 1, 1968.

8 Smalley, A. J., Vohr, J. H., Castelli, V., and Wachmann, C., "An Analytical and Experimental Investigation of Turbulent Flow in Bearing Films Including Convective Fluid Inertial Forces," ASME JOURNAL OF LUBRICATION TECHNOLOGY, Vol. 96, No. 1, 1974, pp. 151–157.

9 Galetuse, S., "Experimental Study on the Interference of Inertia and Friction Forces in Turbulent Lubrication," ASME JOURNAL OF LUBRICATION TECHNOLOGY, Vol. 96, No. 1, 1974, pp. 164–167.

10 Burton, R. A., Carper, H. J., and Hsu, Y. C., "An Experimental Study and Analysis of Turbulent Film Tilted Pad Bearings," ASME JOURNAL OF LUBRICATION TECHNOLOGY, Vol. 96, No. 1, 1974, pp. 168–173.

11 Gregory, R. S., "Performance of Thrust Bearings at High Operation Speeds," ASME JOURNAL OF LUBRICATION TECHNOLOGY, Vol. 96, No. 1, 1974, pp. 7–14.

12 Pan, C. H. T., "Calculation of Pressure, Shear, and Flow in Lubrication Films for High Speed Bearings," ASME JOURNAL OF LUBRICATION TECHNOLOGY, Vol. 96, No. 1, 1974, pp. 80–94.

13 Constantinescu, V. N., and Galetuse, S., "On the Possibilities of Improving the Accuracy of the Evaluation of Inertia Forces in Laminar and Turbulent Films," ASME JOURNAL OF LUBRICATION TECHNOLOGY, Vol. 96, No. 1, 1974, pp. 69–79.

14 Tipei, N., "Flow Characteristics and Pressure Head Build-up at the Inlet of Narrow Passages," ASME JOURNAL OF LUBRICATION TECHNOLOGY, Vol. 100, No. 1, 1978, pp. 47–55.

15 Burton, R.A., and Carper, J. H., "An Experimental Study of Annular Flows with Applications in Turbulent Flow Lubrication," ASME JOURNAL OF LUBRICATION TECHNOLOGY, Vol. 89, No. 3, 1967, pp. 381–389.

16 Launder, B. E., and Leschziner, M., "Flow in Finite-Width Thrust Bearings Including Inertial Effects 1, Laminar Flow," ASME JOURNAL OF LUBRICATION TECHNOLOGY, Vol. 100, July 1978, pp. 330–338.

17 Elrod, H. G., Anwar, I., and Colsher, R., "Transient Lubricating Films with Inertia," ASME JOURNAL OF LUBRICATION TECHNOLOGY, Vol. 105, July 1983, pp. 369–374.

18 Pinkus, O., and Sternlicht, B., *Theory of Hydrodynamic Lubrication*, McGraw-Hill, New York, 1961, pp. 352–357.

19 Hays, D., "Plane Sliders of Finite Width," *Trans. ASLE*, Vol. 1, No. 2, 1958, pp. 233–240.